ACADEMIA ROMÂNĂ
Revue Roumaine de Chimie
https://www.icf.ro/rrch/

Rev. Roum. Chim.,
2023, *68*(7–8), 339–345
DOI: 10.33224/rrch.2023.68.7-8.03

Dedicated to Dr. Niculae I. Ionescu on the occasion of his 90th anniversary

ADSORPTION PROPERTIES OF BORON NITRIDE: A PROMISING MATERIAL FOR DEPOLLUTION APPLICATIONS

Anca VASILE, Florica PAPA, Daniela C. CULITA, Oana Catalina MOCIOIU, Simona PETRESCU, Paul CHESLER, Cristian HORNOIU and Veronica BRATAN*

"Ilie Murgulescu" Institute of Physical Chemistry of the Roumanian Academy, Spl. Independentei 202, Bucharest, Roumania

Received November 29, 2022

The interest in boron nitride (BN) materials has progressively increased due to their special properties such as high chemical stability and non-toxicity. The synthesis of the BN-based materials, starting from boric acid, urea (BN-u) and boric acid and melamine (BN-m) was presented. The obtained materials were characterized by BET, IR Spectroscopy, DR UV-Vis analysis, and Scanning Electron Microscopy (SEM). The synthesized BNs have a high surface area (538.0 m^2/g for BN-u and 994 m^2/g for BN-m) and large pore volume. However, even the material obtained starting from melamine presents a large pore volume, the pore size is higher for BN obtained from urea making it suitable for dye adsorption from wastewater. For this purpose, its performances in adsorption of Brilliant Blue FCF dye, as a model for dye molecules, were studied. The maximum adsorbed quantity of 24.8 mg/g was calculated based on Sips isotherm. The materials were also tested for CO_2 adsorption, with promising results.

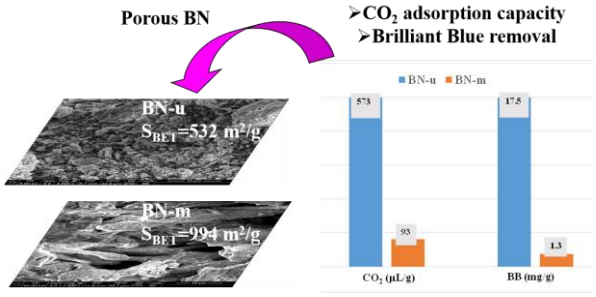

INTRODUCTION

Adsorption is one of the most important techniques used in order to remove contaminants from the environment; because it is safe, simple to use, and implies low costs. In this process the contaminants are transferred from a solution or gaseous mixture to the surface of the solid adsorbent, being mediated by physical or chemical interactions. For the process to succeed, the solid adsorbent has to present a high surface area and pore volume. Among the adsorbents often used today are zeolites,[1,2] clays[3,4] or activated carbon, commercially available or obtained from different waste materials.[5,6]

Recent studies reported the use of a new material, namely porous boron nitride (BN), for removing organic molecules (*e.g.*, dyes, pharmaceutical molecules, oils) from water[7-13] or capturing CO_2 from the air.[14,15] Porous BN is non-toxic and possesses high chemical resistance (*e.g.* crystallized h-BN not being attacked by water or any mineral acids except hydrogen fluoride), thermal stability (up to 800–1000 °C in air and more than 2000 °C in an inert atmosphere), mechanical strength, and thermal conductivity.[16,18] BN crystallographic structure is comparable to that of carbon allotropes: cubic-BN (c-BN), with a structure similar to the carbon atoms' arrangement in the diamond crystal; and hexagonal-BN form,

* Corresponding author: vbratan@icf.ro

similar to graphite structure.[18] However, the polarity of B-N bonds makes boron nitride properties different from that of carbonaceous materials. An important difference is the hydrophobicity of BN materials, which can be particularly advantageous for the adsorption of organic molecules from the vapor or the liquid phase.[7] The higher stability towards oxidation of BN materials compared with carbon, is another advantage, being more easier to reactivate and reuse.

Synthesis of porous BN materials with a high specific surface area was recently reported in the literature, and started from different precursors, with or without templates, and various thermal treatments. Marchesini *et al.*[7] used boric acid and urea/melamine in different ratios as precursors; Rushton *et al.*[19] synthesized porous BN by chemical vapor deposition (CVD) and nitridation of ammonia borane using SBA-15 as a hard template. Maiti et al.[20] synthesized porous BN with cotton flower-like morphology and high surface areas from melamine/boric acid as precursors, at 1100 ^{o}C in the presence of N_2/H_2. Wu *et al.*[21] studied the effect of different solvents on the specific surface area of hexagonal boron nitride nanosheets obtained starting from urea and boric acid. In this study, porous BN was synthesized starting from boric acid-urea and boric acid-melamine precursors, at low temperatures, this being one of the simplest and low-cost synthesis methods, which represents the novelty factor of this paper together with the promising results obtained for organic pollutants and CO_2 adsorption.

RESULTS AND DISCUSSION

Figure 1 presents the FTIR spectra recorded in the 400–4000 cm^{-1} range for the obtained materials and they confirm the formation of BN. The FT-IR was used to further explore the functional groups on the surface of both BN samples. FTIR spectra reveal that both samples show typical in-plane B-N bending vibration located at around 1398 cm^{-1} and out-of-plane B-N-B bending vibration at nearly 800 cm^{-1}.[22] The broad bands at 3230 cm^{-1} and 3404 cm^{-1} are due to the ν O-H stretching vibration in B–OH and ν N-H symmetric stretching vibration in B–NH_2, surface bonds arising from the moisture adsorbed on the surface.[23,24] Other absorption peaks that appear in the spectra were ascribed as follows: ν C=O (1650 cm^{-1}) and B-O stretching (1106 cm^{-1}).[25,26]

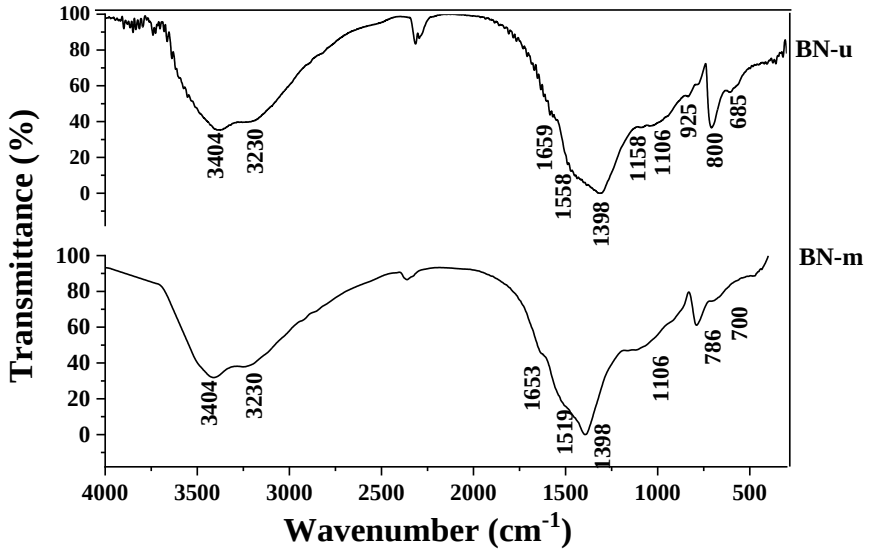

Fig. 1 – FTIR spectra of the prepared BN samples.

Scanning electron microscopy (SEM) was used to reveal the morphology of the samples and the results are presented in Fig. 2. BN-u sample micrograph pointed out a porous structure morphology fused together into an interconnected fibers network. The image of the BN-m sample (Fig. 2b) shows agglomerated quasi-spherical nanoparticles into sheet-like aggregates of micropores.

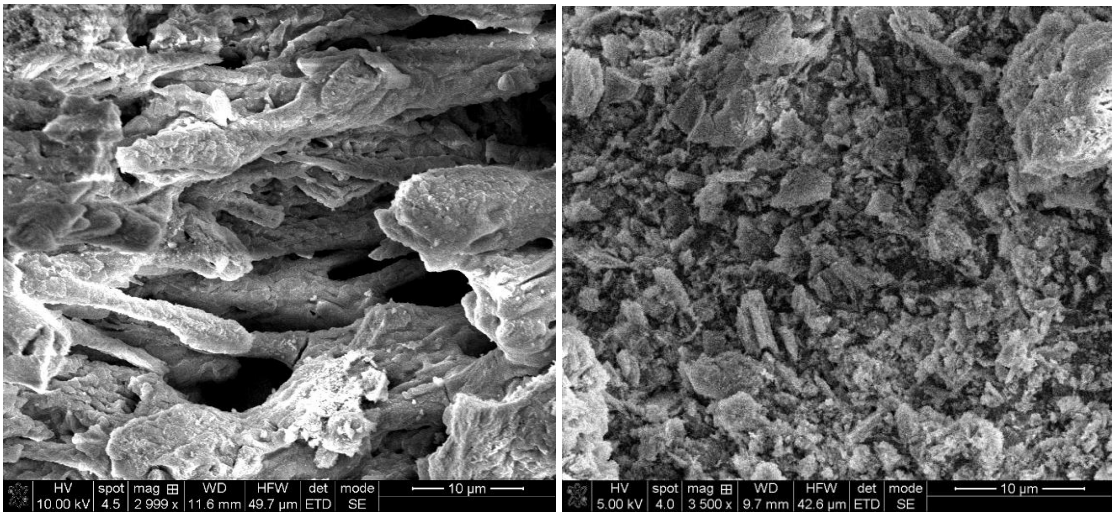

Fig. 2 – SEM images of a) BN-u and b) BN-m samples.

In Fig. 3, nitrogen adsorption–desorption isotherms of boron nitride materials are represented. The sorption isotherms present a typical *type IV* isotherm pattern, based on the IUPAC classification with an H3 hysteresis loop in the relative pressure range of 0.4–1.0, indicating the existence of mesopores. In the case of BN-m, the pattern of the isotherm presents a sharper rise in the low relative partial pressure region. This is an indication of the existence of a micropore fraction, which is responsible for the enhancement of its surface area (Table 1).

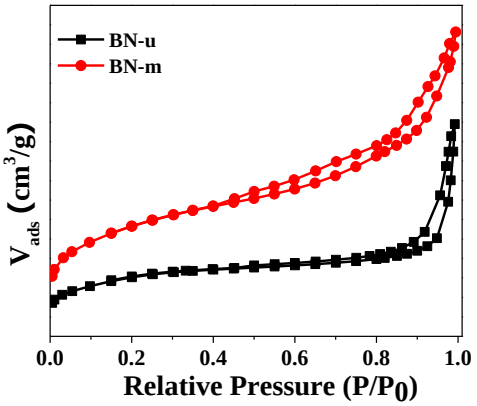

Fig. 3 – N_2 adsorption-desorption isotherms for BN-u and BN-m materials.

The calculated S_{BET} values are high for both samples: 532 m^2/g for BN-u and 994 m^2/g for BN-m, respectively. BN-m material presents a larger specific surface area and total pore volume than that of BN-u (1.2 *vs* 0.84 cm^3/g); still, its main pore diameter is lower (Table 1), which is in concordance with the morphology resulting from SEM images (Fig. 2).

Table 1

The textural properties of the samples

Sample	S_{BET} (m^{2}g^{-1})	V_{total} (cm^{3}g^{-1})	Pore size (nm)
BN-u	532	0.842	10.80
BN-m	994	1.209	6.36

The light absorption in the UV-Vis domain depends on the electronic state of the materials and is used to determine the band gap of semiconductors. Pristine BN has a wide indirect band gap energy of around 5.5 eV, but the reported values are largely dispersed, strongly depending on the morphology and size of the different BN particles.[22,27,28] The UV-Vis spectra registered for prepared BN samples (Fig. 4) exhibit two UV-absorption peaks at 210 nm and 250 nm, and an additional peak at 320 nm for BN-m. Guo *et al.*[22] found that the absorption bands at a higher wavelength (250 and 320 nm) could be related not only to the nanostructure of the BN sample but also to the hydroxylation of the sample. Based on theoretical calculations, they found that the presence of OH groups modifies the HOMO orbital of the material (composed of 2*p* orbitals of *N* atoms).

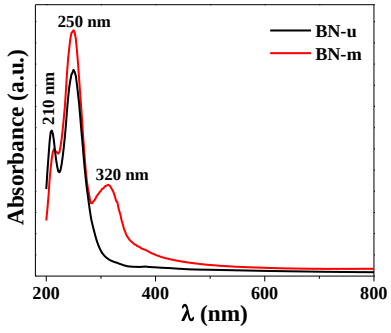

Fig. 4 – UV-Vis spectra of boron nitride materials.

The CO_2 adsorption capacity of the BN materials was measured at room temperature. Pulses of CO_2, each with an injected volume of 100 µL, were performed in six cycles for both BN samples. Surprisingly, BN-u adsorbs significantly more CO_2 than BN-m (Table 2), even though it has a smaller specific surface area, most likely due to its higher porosity. BN-m presents a lower CO_2 capture than BN-u, having a larger proportion of smaller pores that did not allow the adsorption of CO_2 in the pores, which is mainly physically adsorbed on the surface.

Table 2

The CO_2 adsorption capacity parameters of the samples

Sample	Total Volume Adsorbed (µL)	Specific Volume Adsorbed (µL/g)	Monolayer Uptake Volume (µmol/g)
BN-u	31.5	572.9	25.9
BN-m	5.1	93.0	4.2

The BN samples were also tested for removal of Brilliant Blue FCF from the aqueous solution. Initially, the effect of adsorbent dosage on the adsorption efficiency of the BN-u sample was studied and the results were revealed in Fig. 5. It could be observed that the efficiency values increase with the increase of the BN amount, this behavior being related to a higher number of available sites for adsorption. At an adsorbent dosage value of 500 mg/L, a saturation value of efficiency is observed, probably due to the overlapping of the adsorption sites at high amounts of BN.[29]

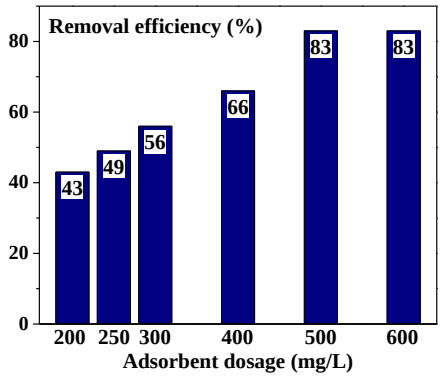

Fig. 5 – The effect of the adsorbent dosage on the removal of the Brilliant Blue FCF from aqueous solution ("adsorbent: BN-u sample; concentration of BB solution; 10 mg/L; time frame: 90 min").

In order for an adsorbent to be effective, it is necessary, in addition to a high adsorption capacity, for the process to reach equilibrium quickly. Thus, the effect of contact time on the adsorption process was followed and the results are presented in Fig. 6. It could be observed that the equilibrium is quickly reached; however, 89 % of BB is removed within 90 min when BN-u was used, compared with only 8% adsorbed on BN-m in the same conditions. BN-u possesses not only a high surface area, but also a mesoporous structure, which provides void volume, offering a higher number of active sites for enhanced BB adsorption, compared with BN-m. The results are consistent with CO_2 adsorption measurements.

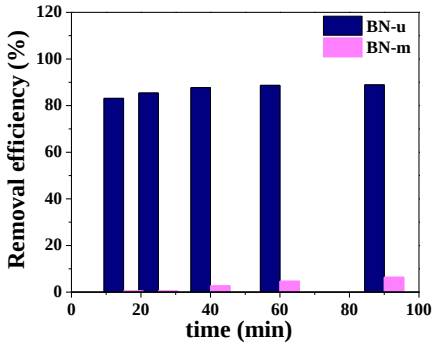

Fig. 6 – The effect of contact time on the BB removal efficiency for BN materials (adsorbent dosage: 500 mg/L; BB solution: 10 mg/L).

In order to obtain information about the possible mechanism of adsorption, as well as the rate-determining step, the time-dependent adsorption behavior of the BN-u sample was analyzed by utilizing the linear form of the pseudo-first-order (PFO) and pseudo-second-order (PSO) kinetic models. An adsorption process will follow one or other of them depending on some factors. Thus, a PFO-type kinetic model will be involved if one of the following conditions is met: 1) the process is at the beginning of the adsorption, 2) the initial concentration of the adsorbate is very high or 3) the adsorbent has a low number of active centers. Conversely: for small C_0, an adsorbent with a high concentration of active centers or/and a process close to equilibrium, the adsorption is described sooner by a PSO-type model. In some cases, the PFO model is involved when the external/internal diffusion is the limiting step, while in the case of the PSO process, the adsorption kinetics is dominated by the adsorption onto active sites.[30] The validity of these kinetic models was studied based on the regression coefficients and on the predicted q_e values. The best correlation was obtained for the pseudo-second-order kinetic model (Figure 7), which is described by the linear equation:

$$\frac{t}{q_t} = \frac{1}{k_2 q_e^2} + \frac{t}{q_e} \quad (1)$$

where q_t (mg/g) was the quantity of pollutant adsorbed at time t; q_e – the quantity of pollutant adsorbed at equilibrium, and k_2 (g×mg^{-1}×min^{-1}) are the rate constant of the adsorption process.

As observed in the figure, the value of R^2 is extremely high (0.9996), and the calculated amount of adsorbed dye (17.6 mg/g) is close to the experimental value (17.3 mg/g).

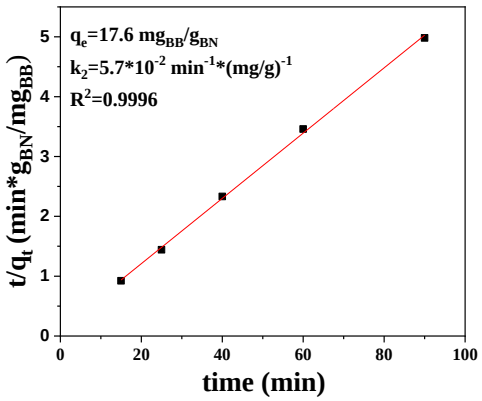

Fig. 7 – Pseudo-second order plots for uptake of BB onto BN-u sample (adsorbent dosage: 500 mg/L; BB solution: 10 mg/L)

Adsorption isotherms are equilibrium relationships that describe how the organic molecules are distributed between the liquid and solid phases, being necessary for optimizing the adsorption process. They also make possible the comparison of the behavior of different adsorbents related to a given pollutant. Thus, for the sample which was proved to be a good adsorbent, namely BN-u, the adsorption isotherm was also represented (Fig. 8).

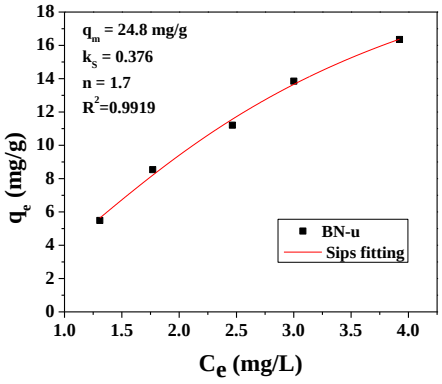

Fig. 8 – Adsorption isotherm of BB on BN-u (initial concentration of BB in the range 5–12 mg/L; adsorbent dosage: 500 mg/L; time to reach the equilibrium: 90 min).

The experimental data were best modeled by the Langmuir-Freundlich (Sips) isotherm, with a correlation coefficient of 0.9919. Sips isotherm is a combination of the Langmuir and Freundlich isotherms: at low concentrations of adsorbate it is reduced at the Freundlich model, and at high adsorbate concentrations it describes the monolayer adsorption associated with a Langmuir isotherm. The mathematical expression of Sips isotherm is:[31]

$$q_e = \frac{q_m \cdot (K_S \cdot C_e)^n}{1 + (K_S \cdot C_e)^n} \quad (2)$$

where C_e (mg/L), q_e (mg/g) represents the aqueous phase concentration and the adsorbed quantity of the adsorbate at the equilibrium, q_m – the maximum adsorption capacity of the adsorbent (mg/g); K_a is the affinity constant for adsorption (L/mg) and n is the index of heterogeneity.

The fitting curve is also introduced in Fig. 8. As resulted from the figure, the maximum Brilliant Blue adsorption capacity of boron nitride obtained from urea is 24.8 mg/g. It has to be noted that porous BN possesses lower adsorption performances than chitosan (210 mg/g),[32] but better adsorption capacity than coir pith carbon[33] (15.24 mg/g) or activated bleaching earth[34] (8.45 mg/g).

EXPERIMENTAL

Synthesis

Two porous BN were synthesized. The first BN (denoted as BN-u) was prepared from Boric Acid: Urea (1:30 weight ratio) mixed in water-ethanol solution (1:1 volume ratio) at 75 ºC, until the solvent evaporated. The obtained solid material was dried at 90 ºC and then thermally treated using the following protocol: heating until 550 ºC (5 ºC/min) in O_2 atmosphere, followed by heating with the same rate to 750 ºC in N_2 atmosphere and maintained at that temperature for 5 hours. The second BN sample was synthesized from Boric Acid: Melamine (1:15 weight ratio) following the same protocol.

Characterization

The as-prepared boron nitride materials were characterized using Fourier transform infrared (FTIR), N_2 physisorption, Scanning Electron Microscopy (SEM), and UV-Vis spectroscopies. The structure of the materials was investigated by FTIR using a Nicolet 6700 with OMNIC software. The equipment resolution is 4 cm^{-1} and the spectra were recorded in the mid-infrared domain. For characterizing the morphological structure of as-prepared samples the SEM Quanta 3D FEG instrument was used. Powders were placed on double-sided carbon tape and investigated without further coating.

The textural analysis of the samples was performed by nitrogen physisorption at –196 ºC using a Micromeritics ASAP 2020 analyzer. Before each measurement, the samples were degassed under vacuum at 300 ºC for 5 h. The specific surface areas (S_{BET}) were calculated using the Brunauer-Emmett-Teller (BET) equation and the total pore volume (V_{total}) was estimated from the amount adsorbed at the relative pressure of 0.99. Diffuse reflectance UV-Vis spectra were recorded in the range 900–200 nm, using a Perkin Elmer Lambda 35 spectrophotometer, equipped with an integrating

sphere. The Kubelka-Munk function was applied to convert the reflectance data into absorption ones.

Adsorption tests

CO_2 adsorption

The CO_2 adsorption capacities were evaluated using pulse chemisorption performed at room temperature with a ChemBet-3000 Quantachrome Instrument, equipped with a thermal conductivity detector (TCD). Prior to CO_2 chemisorption measurements, the adsorbents were pretreated in helium at 200 °C for 30 minutes.

Dye adsorption

The adsorption ability for the removal of dye from aqueous solutions was also determined. As a model for dye, Brilliant Blue FCF (BB) was used. Firstly, dye solutions of different concentrations (5, 6, 8, 10, and 12 mg/L) were prepared by diluting a stock solution (100 mg/L). Then, the effect of the adsorbent amount on the efficiency of the process was followed. In this case, different amounts of BN were mixed with a 10 mL BB solution of 10 mg/L concentration and the efficiency of the adsorption was calculated after 90 min. To determine the influence of contact time, 12.5 mg of the BN sample was added to 25 mL BB aqueous solution (10 mg/L) and stirred together, until no significant changes were observed. All the experiments took place in darkness, at room temperature, without adjusting the pH. The adsorption process was monitored by recording the UV-vis absorption spectra of the aqueous solution with a Perkin Elmer Lambda 35 spectrometer, and measuring the absorbance at 628 nm. For this purpose, 3 mL from the suspension was taken out at different time intervals and the adsorbent was separated from the suspension using a Millipore syringe filter of 0.22 μm.

The adsorption isotherms were obtained in the same manner, mixing and stirring 5 mg BN with 10 mL solution with different initial BB concentrations for 90 minutes, which is enough for attaining the equilibrium state. The removal efficiency (R%), the quantity of dye adsorbed at time t, denoted q_t (mg/g), and the quantity of pollutant adsorbed at equilibrium, q_e, were calculated as follows:

$$R\% = \frac{C_0 - C_e}{C_0} \cdot 100, \quad q_t = \frac{(C_0 - C_t)\cdot V}{w}, \quad q_e = \frac{(C_0 - C_e)\cdot V}{w} \qquad (3)$$

where C_0, C_t, and C_e are the concentrations of the adsorbates at the beginning of the experiment, at time t and, at equilibrium, respectively, and they are measured in mg/L; V – the volume of the adsorbate solution (L), and w –the amount of BN (mg).

CONCLUSIONS

Starting from boric acid/urea, and boric acid/melamine, respectively, two porous BN samples were synthesized at a low temperature. BN formation was confirmed by FTIR spectra. The pores measurements were in concordance with the morphology resulting from SEM and CO_2 capture evaluation tests. BN-u (S_{BET} = 538.0 m^2/g) adsorbs significantly more CO_2 than BN-m (S_{BET} = 994 m^2/g), even though it has a smaller specific surface area, most likely due to its higher porosity. 89 % of Brilliant Blue is removed within a 90 min time frame when BN-u was used, compared with only 8% adsorbed on BN-m under the same conditions. From Sips isotherm a maximum quantity of BB adsorbed on the BN-u sample was evaluated at 24.8 mg/g, which is higher than some other values reported in the state-of-the-art, making it a suitable candidate for the treatment of wastewater.

REFERENCES

1. B. Armagan and M. Turan, *Desalination*, **2004**, *70*, 33–39.
2. P. Misaelides, *Microporous Mesoporous Mater*., **2011**, *144*, 15–18.
3. A. Kausar, M. Iqbal, A. Javed, K. Aftab, H. N. Bhatti and S. Nouren, *J. Mol. Liq.*, **2018**, *256*, 395–407.
4. A. A. Adeyemo, I. O. Adeoye and O. S. Bello, *Appl. Water Sci.*, **2017**, *7*, 543–568.
5. F. Mbarki, T. Selmi, A. Kesraoui, M. Seffen, *Ind Crops Prod*, **2022**, *178*, 114546.
6. Y. Yu, N. Qiao, D. Wang, Q. Zhu, F. Fu, R. Cao, R. Wang, W. Liu and B. Xu, *Bioresour. Technol.*, **2019**, *285*, 121340.
7. S. Marchesini, X. Wang, and C. Petit, *Front. Chem.*, **2019**, *7*, 160.
8. D. Liu, W. Lei, S. Qin and Y. Chen, *Sci. Rep.*, **2014**, *4(1)*, 1–5.
9. J. Li, X. Xiao, X. Xu, J. Lin, Y. Huang, Y. Xue, P. Jin, J. Zou and C. Tang, *Sci. Rep.*, **2013**, *3*, 1–7.
10. Y. Chao, J. Zhang, H. Li, P. Wu, X. Li, H. Chang, J. He, H. Wu, H. Li and W. Zhu, *J. Chem. Eng.*, **2020**, *387*, 124138.
11. Q. Li, T. Yang, Q. Yang, F. Wang, K.C. Chou and X. Hou, *Ceram. Int.*, **2016**, *42*, 8754–8762.
12. T. Shen, S. Liu, W. Yan, and J. Wang, *J. Mater. Sci.*, **2019**, *54*, 8852–8859.
13. Q. Song, Y. Fang, Z. Liu, L. Li, Y. Wang, J. Liang, Y. Huang, J. Liu, L. Hu, J. Zhang and C. Tang, *J. Chem. Eng*, **2017**, *325*, 71–79.
14. S. Marchesini, A. Regoutz, D. Payne and C. Petit, *Microporous and Mesoporous Mater.*, **2017**, *243*, 154–163.
15. F. Xiao, Z. Chen, G. Casillas, C. Richardson, H. Li and Z. Huang, *Chem. Comm.*, **2016**, *52*, 3911–3914.
16. G. Postole, M. Caldararu, N. I. Ionescu, B. Bonnetot, A. Auroux and C. Guimon, *Thermochim. Acta*, **2005**, *434*, 150–157.
17. D. Gonzalez-Ortiz, C. Salameh, M. Bechelany and P. Miele, *Mater. Today*, **2020**, *8*, 100–107.
18. M. Mirzaee, A. Rashidi, A. Zolriasatein and M. R. Abadchi, *Ceram. Int.*, **2021**, *47*, 5977–5984.
19. B. Rushton and R. Mokaya, *J. Mater. Chem.*, **2008**, *18*, 235–241.
20. K. Maiti, T. D. Thanh, K. Sharma, D. Hui, N. H. Kim and J. H. Lee, *Compos. B Eng.*, **2017**, *123*, 45e54.
21. P. Wu, W. Zhu, Y. Chao, J. Zhang, P. Zhang, H. Zhu, C. Li, Z. Chen, H. Li and S. Dai, *Chem. Comm.*, **2016**, *52*, 144–147.
22. Y. Guo, R. Wang, P. Wang, L. Rao and C. Wang, *ACS Appl. Mater. Interfaces.*, **2018**, *10*, 4640–4651.
23. B. Yu, W. Xing, W. Guo, S. Qiu, X. Wang, S. M. Lo and Y. Han., *J. Mater. Chem. A,*, **2016**, *4*, 7330–7340.
24. P. Dibandjo, L. Bois, F. Chassagneux and P. Miele, *J. Eur. Ceram. Soc.*, **2007**, *27*, 313–317.
25. P. Gross and H. A. Höppe, *Chem. Mater.*, **2019**, *31*, 8052–8061.
26. S. Mondal and A. K. Banthia, *Adv. Mater. Res.*, **2007**, *29*, 199–202.

27. R. Gao, L. Yin, C. Wang, Y. Qi, N. Lun, L. Zhang, Y.-X. Liu and X. Wang, *J. Phys. Chem. C*, **2009**, *113*, 15160–15165.
28. Y. C. Zhu, Y. Bando, D. F. Xue, T. Sekiguchi, D. Golberg, F. F Xu and Q. L. Liu, *J. Phys. Chem. B*, **2004**, *108*, 6193.
29. M. Ghaedi, A. Golestani Nasab, S. Khodadoust, M. Rajabi and S. Azizian, *J. Ind. Eng. Chem*,, **2014**, *20*, 2317–2324.
30. J. Wang and X. Guo, *J. Hazard. Mater*., **2020**, *390*, 122–156.
31. G. P. Jeppu and T. P. Clement, *J. Contam. Hydrol.*, **2012**, *129*, 46–53.
32. G. L. Dotto and L. D. A. Pinto, *Carbohydr. Polym*., **2011**, *84*, 231–238.
33. D. Kavitha and C. Namasivayam, *Chem. Eng. J.*, **2008**, *139*, 453–461.
34. W. T. Tsai, C. Y. Chang, C. H. Ing and C. F. Chang, *J. Colloid. Interface Sci.*, **2004**, *275*, 72–78.